

Explosive Percolation Obeys Standard Finite-Size Scaling in an Event-based Ensemble

Ming Li,^{1,*} Junfeng Wang,¹ and Youjin Deng^{2,3,†}

¹*School of Physics, Hefei University of Technology, Hefei, Anhui 230009, China*

²*Hefei National Laboratory for Physical Sciences at Microscale and Department of Modern Physics, University of Science and Technology of China, Hefei, Anhui 230026, China*

³*MinJiang Collaborative Center for Theoretical Physics, College of Physics and Electronic Information Engineering, Minjiang University, Fuzhou, Fujian 350108, China*

(Dated: April 6, 2023)

Explosive percolation in the Achlioptas process, which has attracted much research attention, is known to exhibit a rich variety of critical phenomena that are anomalous from the perspective of continuous phase transitions. Hereby, we show that, in an event-based ensemble, the critical behaviors in explosive percolation are rather clean and obey the standard finite-size scaling theory, except for the large fluctuation of pseudo-critical points. In the fluctuation window, multiple fractal structures emerge and the values can be derived from a crossover scaling theory. Further, their mixing effects account well for the previously observed anomalous phenomena. Making use of the clean scaling in the event-based ensemble, we determine with a high precision the critical points and exponents for a number of bond-insertion rules, and clarify ambiguities about their universalities. Our findings hold true for any spatial dimensions.

Percolation is one of the paradigms in statistical physics and probability theory [1]. The standard percolation model on a lattice is defined by randomly occupying sites or bonds with some probability, and undergoes a continuous phase transition. Simple alterations of the percolation, such as lattice type, only result in different critical points, and do not change the universality class [1]. By adopting significantly different percolation rules, such as rigidity percolation [2, 3], new universalities can arise. Nevertheless, the continuity of the transition remains robust, and the finite-size scaling (FSS) theory is always applicable.

In recent years, there has been an ongoing discussion on the so-called Achlioptas process [4, 5], in which some intrinsic mechanism is introduced to suppress the growth of large clusters. A basic way is called the product rule [6]. At each time step, two empty bonds are randomly picked up, the size-product of the two clusters containing the ending sites of each bond is calculated, and the one, leading to a smaller size-product, is inserted. As a consequence, the onset of percolation is significantly delayed, but once it happens, a large cluster emerges suddenly, hence the name explosive percolation (EP). EP has been observed in a wide class of Achlioptas processes, including on regular lattices [7, 8] and scale-free networks [9, 10], and in systems with other bond-insertion rules [11–15]. EP was perceived as a discontinuous transition when it was introduced [6–11, 13, 16, 17], but later studies suggested that the sharp transition is continuous, despite displaying rich anomalous behaviors [12, 18–22].

Consider the largest cluster C_1 , whose relative size, $m \equiv \langle C_1 \rangle / N$ (N is the system volume), acts as an order parameter. According to the FSS theory, at the critical point T_c , m scales as N^{d_f-1} , where d_f is the fractal dimension with respected to the system volume N [23]. Further, the probability distribution of C_1 can be renormalized to a single-variable function as $P(C_1, N) dC_1 = P(x) dx$, with $x \equiv C_1 / N^{d_f}$. However, as in Fig. 1(a) for random graphs, EP displays a bimodal distribution [19, 24], and, further, multiple fractal dimensions

emerge—i.e., different values, d_f^+ and d_f^- , are needed to collapse the data for different peaks. Actually, neither of them is the correct fractal dimension, as we shall show later.

The FSS theory also tells us that $C_1 = N^{d_f} \tilde{m}(\delta T N^{1/\nu})$, where $\delta T = T - T_c$, ν is the correlation-length exponent with respected to the system volume N , and $\tilde{m}(\cdot)$ is a universal function. However, a wide range of ν values, inconsistent within the quoted errors, has been reported for EP [18, 19, 25–27]. It was further observed [19, 28] that there simultaneously exists a pair of exponents, $\nu_1 < \nu_2$, but neither of them is sufficient to describe the scaling of C_1 data near T_c , see Fig. 1(b,c). Other anomalous phenomena include the powder-keg mechanism [11], non-self-averaging property [15], and hysteresis [29]. It seems that, despite being continuous, EP does not obey the standard FSS theory, and extracting correct exponents becomes difficult. This leads to controversies about how the universality of EP depends on bond-insertion rules.

By dynamically recording $C_1(t)$, where time step t is also the number of inserted bonds, the event, $\mathcal{T}_N \equiv t_{\max}/N$, can be located by the maximum point t_{\max} of the incremental size, $C_1(t) - C_1(t-1)$ [14, 18, 30]. Major progress was recently achieved [28], in which the pseudo-critical point $T_N \equiv \langle \mathcal{T}_N \rangle$ and the variance $\sigma_T^2 \equiv \langle \mathcal{T}_N^2 \rangle - \langle \mathcal{T}_N \rangle^2$ are calculated. The correct fractal dimension for random graphs, $d_f = 0.935$, was obtained at \mathcal{T}_N . It was further observed that the deviation decays as $T_N - T_c \sim N^{-1/\nu_1} = N^{-0.75}$ but the fluctuation vanishes more slowly as $\sigma_T \sim N^{-1/\nu_2} = N^{-0.50}$. The authors concluded that ν_2 serves as the correlation-length exponent of EP.

In this Letter, we study EP in a similar way as in [14, 18, 28, 30, 31]. A simple but important difference is that, after locating \mathcal{T}_N , the process was repeated according to the recorded sequence of inserted bonds. This allows us to sample any quantity at any time step. Here, we focus on two basic quantities—the order parameter m , and the susceptibility $\chi \equiv \langle \sum_{i \neq 1} C_i^2 \rangle / N$. From the total number of clusters with size in $[s, s + \Delta s]$, we also calculate the cluster-number density $n(s, N)$. By definition, one has $\chi = \sum_s s^2 n(s, N)$. We explore the scaling behav-

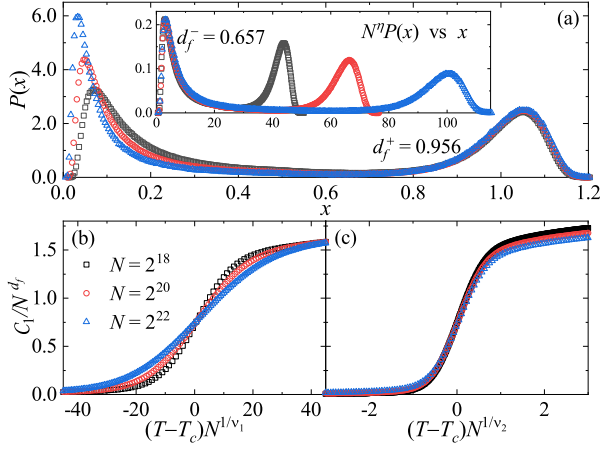


FIG. 1. Anomalous scaling behaviors in the conventional ensemble. (a) The bimodal distribution $P(x)$ of the largest-cluster size C_1 at T_c . Data collapse around the right peak is achieved by defining $x = C_1/N^{d_f^+}$ with $d_f^+ = 0.956$, while for the left peak, one has to use a smaller value $d_f^- = 0.657$ and a rescaled exponent $\eta = 0.08$. (b, c) The scaling of C_1 near T_c , with the exponents $1/\nu_1 = 0.740$ and $1/\nu_2 = 0.500$ (the correct fractal dimension $d_f = 0.935$ is used here). The data collapse is somewhat better for ν_2 , which was incorrectly regarded as the correlation-length exponent [19, 28].

iors of these quantities, and their dependence on the dynamic deviation $\delta\mathcal{T} \equiv T - \mathcal{T}_N$. To distinguish from the conventional ensemble of fixed bond density, we call such dynamic sampling to be in the event-based ensemble.

We perform extensive simulations on random graphs and on hypercubic lattices in dimensions from 2 to 6, and observe the following. First, we find that, at \mathcal{T}_N and in terms of $\delta\mathcal{T}$, the standard FSS theory applies well to any quantity as $Q(T, N) = N^Y \tilde{Q}(\delta\mathcal{T}N^{1/\nu_1})$, with Y the associated exponent. Note that the correlation-length exponent is unique, which is ν_1 instead of ν_2 . Second, we reveal that the previously observed exponents d_f^\pm , correspond to the fractal dimensions in the fluctuation window $O(N^{-1/\nu_2})$ at the super- and sub-critical sides of \mathcal{T}_N , respectively. Moreover, we propose a crossover scaling theory and derive the values of d_f^\pm . All these findings hold true for any dimension and a number of bond-insertion rules. Finally, we determine with a high precision the percolation threshold and the critical exponents for a number of bond-insertion rules, and identify their universalities. For clarity, herein we only present the numerical results for the basic EP (with the product rule) on random graphs, and will publish other results elsewhere [32].

Standard finite-size scaling in the event-based ensemble.— The probability distribution of C_1 at \mathcal{T}_N , is displayed in Fig. 2(a). In contrast to Fig. 1(a), the distribution is smooth and has a single peak, and, more importantly, it can be expressed as a single-variable function as $P(x = C_1/N^{d_f})$. Note that the correct fractal dimension, $d_f = 0.935$, equals neither to d_f^+ nor d_f^- . In standard percolation, the cluster-number density at criticality follows a power-law behavior up to a cutoff size $s_N \sim N^{d_f}$, i.e., $n(s, N) = s^{-\tau} \tilde{n}(s/s_N)$, and the Fisher expo-

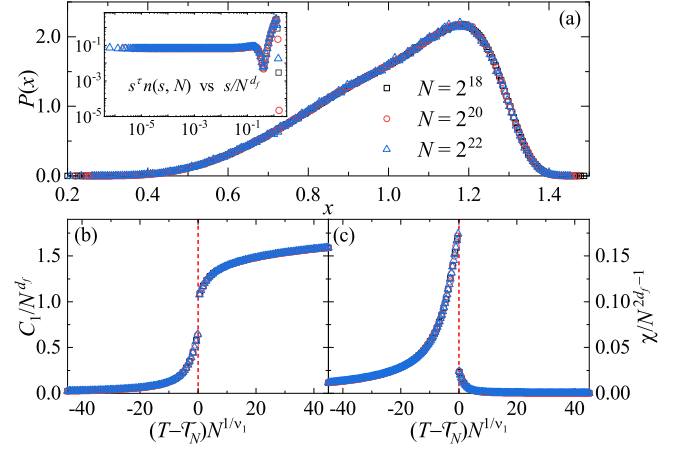


FIG. 2. Standard FSS behaviors in the event-based ensemble. (a) At \mathcal{T}_N , C_1 has a uniform distribution $P(x = C_1/N^{d_f})$, where the correct fractal dimension is $d_f = 0.935$ instead of d_f^+ or d_f^- . The inset shows that the cluster-number density obeys $n(s, N) = s^{-\tau} \tilde{n}(s/N^{d_f})$, with $\tau = 1 + 1/d_f \approx 2.07$. (b, c) Over a wide range at both sides of \mathcal{T}_N , the standard FSS form holds well for C_1 and susceptibility χ , where the jump arises from the event-based definition of \mathcal{T}_N . The correct correlation-length exponent is $1/\nu_1 = 0.740$, instead of $1/\nu_2 = 0.500$ [19, 28].

nent τ satisfies the hyperscaling relation $\tau = 1 + 1/d_f$. For EP, this gives $\tau = 2.07$ from $d_f = 0.935$, and the nice data collapse in the inset of Fig. 2(a) clearly demonstrates that $n(s, N)$ for EP obeys the standard FSS form.

Following the standard FSS ansatz, we plot, respectively in Fig. 2(b) and (c), the largest cluster C_1 and the susceptibility χ versus the renormalized dynamic deviation $z \equiv \delta\mathcal{T}N^{1/\nu_1}$, where $d_f = 0.935$ and $1/\nu_1 = 0.740$. Excellent data collapse is achieved over a wide range of z , which strongly supports that, despite of being sharp, EP is a continuous transition and obeys the standard FSS theory.

To determine the percolation threshold T_c and the critical exponents, d_f and $1/\nu_1$, we fit data to the standard FSS ansatz

$$T_N = T_c + N^{-1/\nu_1}(b_0 + b_1 N^{-\omega_1} + b_2 N^{-\omega_2}), \quad (1)$$

$$C_1 = N^{d_f}(a_0 + a_1 N^{-\omega_1} + a_2 N^{-\omega_2}), \quad (T = \mathcal{T}_N) \quad (2)$$

where the terms with ω_i ($i = 1, 2$) are for finite-size corrections. We obtain $T_c = 0.8884491(2)$, $d_f = 0.935(1)$ and $1/\nu_1 = 0.740(2)$, where systematic errors have been taken into account.

Fluctuation window and multiple fractal dimensions.— For standard percolation, the deviation and the fluctuation of \mathcal{T}_N are in the same order, $T_N - T_c \sim \sigma_T \sim N^{-1/\nu_1}$, where exponent ν_1 is unique. For EP, however, σ_T vanishes with a much slower speed and is governed by another exponent as $\sigma_T \sim N^{-1/\nu_2}$ [28]. The fit of the σ_T data gives $1/\nu_2 = 0.503 \approx 1/2$, and the inequality, $\nu_1 < \nu_2$, is clearly shown in Fig. 3(a). Thus, beyond the standard scaling window $O(N^{-1/\nu_1})$, a fluctuation window $O(N^{-1/\nu_2})$ is well defined.

We sample observables at $\mathcal{T}_N^\pm \equiv \mathcal{T}_N \pm aN^{-1/\nu_2}$ and set $a = 1$ for simplicity. The largest-cluster sizes, C_1^\pm , are also well de-

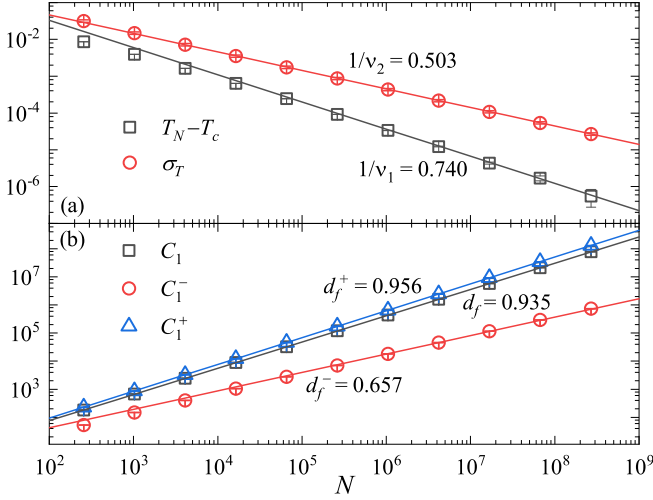


FIG. 3. Multiple critical exponents as determined by the standard FSS ansatz. (a) The deviation is $T_N - T_c \sim N^{-1/\nu_1}$ with $1/\nu_1 = 0.740(2)$, but the fluctuation is $\sigma_T \sim N^{-1/\nu_2}$ with $1/\nu_2 = 0.503(3)$. The fluctuation window $O(N^{-1/\nu_2})$ is larger than the standard scaling window $O(N^{-1/\nu_1})$, implying a non-self-averaging effect in the conventional ensemble. (b) The largest clusters, C_1 at \mathcal{T}_N , C_1^- in the fluctuation window $O(N^{-1/\nu_2})$ for $T > \mathcal{T}_N$ and $T < \mathcal{T}_N$, respectively. It is shown that, while C_1 has the fractal dimension $d_f = 0.935(1)$, C_1^- have $d_f^+ = 0.956(2)$ and $d_f^- = 0.657(3)$, respectively.

scribed by a power-law scaling (Fig. 3(b)). The fits by Eq. (2) give $d_f^+ = 0.956(3)$ for \mathcal{T}_N^+ and $d_f^- = 0.657(3)$ for \mathcal{T}_N^- , which agree well with those in Fig. 1(a). This means that the two peaks in Fig. 1(a) actually correspond to the scaling behaviors in the fluctuation window, respectively at the super- and sub-critical sides. It is thus revealed that the critical behaviors in the conventional ensemble are effectively a mixture of those in the fluctuation window.

The pseudo-critical points \mathcal{T}_N typically deviate away from the thermodynamic point T_c by an amount of $O(N^{-1/\nu_2})$, while the correct critical behaviors are around \mathcal{T}_N within a narrow window $O(N^{-1/\nu_1})$. In terms of $z = \delta\mathcal{T}N^{1/\nu_1}$, the fluctuation window is infinitely large as $|z| \sim N^{1/\nu_1-1/\nu_2} \rightarrow \infty$. This suggests that the mixing effect is over an infinite range, and cannot be averaged out by taking more samples. It is thus no surprising that anomalous critical phenomena arise at T_c .

Relation between multiple fractal dimensions.— From the scaling behaviors in Fig. 2, we expect that $d_f = 0.935$ is the only correct fractal dimension and d_f^\pm can be derived. According to the FSS theory, the correlated size behaves as $\xi_s \sim |\delta\mathcal{T}|^{-\nu_1}$, so that $|z| = |\delta\mathcal{T}|N^{1/\nu_1} \sim (N/\xi_s)^{1/\nu_1}$. In the fluctuation window, which has $N \gg \xi_s$ from $z \rightarrow \infty$, the thermodynamic scaling should be recovered.

Let us consider the crossover scaling from finite- to infinite- N . For susceptibility, as $|z|$ increases, $\chi = N^{2d_f-1}\tilde{\chi}(z)$ should gradually evolve to $\chi \sim |\delta\mathcal{T}|^{-\gamma}$. To eliminate finite- N dependence, it is requested that $\tilde{\chi}(|z| \rightarrow \infty) \sim |z|^{-\gamma}$ with $\gamma/\nu = 2d_f - 1$. The thermodynamic correspondence of C_1 is the order parameter $m = N^{d_f-1}\tilde{m}(z)$. For a continuous phase transition and for

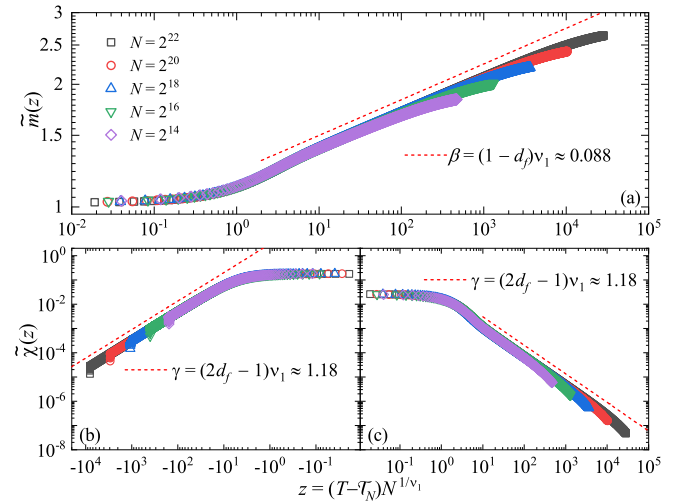


FIG. 4. Crossover scaling behaviors in terms of the renormalized dynamic distance $z \equiv \delta\mathcal{T}N^{1/\nu_1}$. (a) The universal function $\tilde{m}(z)$ in the FSS of the order parameter, $m = N^{d_f-1}\tilde{m}(z)$, scales as $\tilde{m}(z \rightarrow \infty) \sim z^\beta$ in the super-critical side, with $\beta = (1 - d_f)\nu_1 \approx 0.088$. (b, c) The universal function $\tilde{\chi}(z)$ in the FSS of the susceptibility, $\chi = N^{2d_f-1}\tilde{\chi}(z)$, scales as $\tilde{\chi}(|z| \rightarrow \infty) \sim |z|^{-\gamma}$ with $\gamma = (2d_f - 1)\nu_1 \approx 1.18$, which holds true at both the sub-critical ($z < 0$) and the super-critical ($z > 0$) sides of \mathcal{T}_N .

infinite- N , m remains zero for $\delta\mathcal{T} < 0$ and the long-range order is continuously developed as $(\delta\mathcal{T})^\beta$ for $\delta\mathcal{T} > 0$. In the super-critical phase, the crossover scaling of $\tilde{m}(z)$ can be extracted as $\tilde{m}(z \rightarrow \infty) \sim z^\beta$ with $\beta/\nu = 1 - d_f$. These are well supported by Fig. 4.

From $C_1 = N^{d_f}\tilde{m}(z)$, $\tilde{m}(z) \sim z^\beta$ and $z \sim N^{1/\nu_1-1/\nu_2}$, the d_f^+ value is readily calculated as $d_f^+ = 1 - (1 - d_f)(\nu_1/\nu_2) \approx 0.956$, in excellent agreement with those in Figs. 1(a) and 3(b). At the sub-critical side, from the correlated size $\xi_s \sim |\delta\mathcal{T}|^{-\nu_1} \sim N^{\nu_1/\nu_2}$, we expect $C_1^- \sim \xi_s^{d_f^-} \sim N^{d_f^-(\nu_1/\nu_2)}$, giving $d_f^- = d_f(\nu_1/\nu_2) \approx 0.632$. This is somewhat smaller than $d_f^- = 0.657$ in Figs. 1(a) and 3(b), and it can be explained by an alternative way based on χ and $n(s, N)$.

Consider a sub-critical window $O(N^{-1/\lambda})$ centered around \mathcal{T}_N , with $\lambda > \nu_1$, we have $\chi \sim N^{(2d_f-1)(\nu_1/\lambda)}$ from the crossover scaling of χ , and expect $n(s, N) = s^{-\tau}\tilde{n}(s/s_\lambda)$, with the cutoff size $s_\lambda \sim N^{d_\lambda} < N^{d_f}$. The number of clusters of size s_λ is diverging, which is $N_\lambda \sim N s_\lambda^{1-\tau} \sim N^{1-(d_\lambda/d_f)}$, with $s^{1-\tau}$ for the cumulative cluster-number density. With this, the leading term of χ can be expressed as $s_\lambda^2 N_\lambda / N \sim N^{2d_\lambda-d_\lambda/d_f}$. Thus, by setting $(2d_f-1)(\nu_1/\lambda) = 2d_\lambda-d_\lambda/d_f$, the relation between d_λ and d_f is established $d_\lambda = d_f(\nu_1/\lambda)$, and $d_f^- = d_f(\nu_1/\nu_2)$ is recovered for $\lambda = \nu_2$. Note that d_λ is to characterize the typical size of a diverging number of clusters, while C_1 is the largest one. From the extreme-value theory, one expects $C_1 \sim N^{d_\lambda}(\ln N)^\kappa$, where exponent κ depends on the distribution of cutoff clusters. This explains why the fitting result ($d_f^- = 0.657$) is slightly larger than the predicted value ($d_f^- = 0.632$).

Universities.— Unlike in standard percolation, it is suggested that, for EP, small alteration of bond-insertion rule can lead to different critical exponents [4]. For instance, the

TABLE I. Percolation thresholds T_c and critical exponents for various bond-insertion rules, including the product rule (PR), the sum rule (SUM), the CDGM rule, the best of m rule for $m = 3$ ($m3$), and the additional rule (AD). EP has two basic exponents, the correlation-length exponent ν_1 and the fractal dimension d_f , and, in addition, it has the fluctuation exponent ν_2 . It is argued that the fluctuation obeys the central-limit theorem and thus $\nu_2 = 2$ holds exactly.

Rules	T_c	$1/\nu_1$	d_f	$1/\nu_2$
PR	0.888 449 1(2)	0.740(2)	0.935(1)	0.503(3)
PR+AD	0.888 449 0(4)	0.740(3)	0.935(1)	0.504(3)
SUM	0.860 207(1)	0.80(3)	0.957(5)	0.503(2)
SUM+AD	0.860 206(1)	0.80(3)	0.953(5)	0.500(3)
CDGM	0.923 207 4(3)	0.8181(1)	0.9545(1)	0.500(2)
$m3$	0.964 789 9(1)	0.875(1)	0.979(1)	0.501(1)

basic product rule (PR) can be modified into the sum rule (SUM) [6], which calculates the total size of the two clusters associated with each candidate bond. Further, an additional rule (AD) can be adopted by preferentially inserting the intra-cluster bond [17]. One can also apply the best of m rule, i.e., choose three candidate bonds ($m3$) or even more [11]. On random graphs, the rule of [12], we call it CDGM by combining the initials of the authors' surnames, is applied: choose a pair of random sites and reserve the site in the smaller cluster, repeat the procedure for the second pair, and finally, insert a bond between the two reserved sites. Controversies remain about how the EP universality depends on bond-insertion rules. As an exemplified case, debate still exists whether the AD rule would change the universality of EP [17]; the fractal dimension was even estimated to be larger than the system dimension, which is clearly unphysical [33].

In the event-based ensemble, we study EP for a list of bond-insertion rules, and the results for random graphs are given in Tab. I. We obtain the following: (1) The AD rule does not change the universality, or even the percolation threshold. (2) Universalities are different for the PR, the SUM, and the $m3$ rule; the phase transition seems to be sharpest for the $m3$ rule. (3) The CDGM rule seems to be in the same universality as the SUM rule, within the estimated errors. But its finite-size corrections are significantly smaller and the estimated exponents have much higher precision, which are in excellent agreement with the result of the numerical method [21].

Discussions.— By an event-based method, we find that EP obeys the standard FSS theory. As standard percolation, EP has two basic exponents, the fractal dimension d_f and the correlation-length exponent ν_1 , which can describe well the critical behaviors of any quantities near the pseudo-critical points \mathcal{T}_N . Nevertheless, EP has a large fluctuation of \mathcal{T}_N , which is governed by another exponent $\nu_2 > \nu_1$. This scenario holds true for different bond-insertion rules, and for any dimension [32]. The high-precision estimate of critical exponents enables us to establish the EP universalities for various bond-insertion rules.

The obtained ν_2 values agree well with 2, except for two dimensions where $1/\nu_2 = 0.484(4)$ is slightly smaller than

0.5 [32]. In units of the renormalized dynamic deviation z , the fluctuation of \mathcal{T}_N is infinitely large $N^{1/\nu_1-1/\nu_2}$, implying that the central-limit theorem is satisfied. Thus, the fluctuation may asymptotically be of Gaussian type and $\nu_2 = 2$ holds exactly. On this basis, we argue that ν_2 is merely a fluctuation exponent and cannot act as a correlation-length exponent.

The anomalous phenomena in the conventional ensemble are revealed to be a mixture of critical behaviors over the fluctuation window. Since it is infinitely wide in units of the renormalized deviation, the self-averaging effect is lacking, and this leads to the inequivalence of different ensembles. Moreover, the multiple fractal dimensions are derived based on the crossover scaling from finite- to infinite- N .

The effective event-based method can find broad applications, since large sample-to-sample fluctuations can widely exist in systems like disordered ones [34]. Moreover, the proposed crossover scaling theory may provide important insights for connecting critical behaviors in different ensembles.

The authors acknowledge helpful discussions with Peter Grassberger, Jingfang Fan, and Sheng Fang. The research was supported by the National Natural Science Foundation of China under Grant No. 12275263, and the National Key R&D Program of China (Grant No. 2018YFA0306501).

* lim@hfut.edu.cn

† yjdeng@ustc.edu.cn

- [1] D. Stauffer and A. Aharony, *Introduction to percolation theory*, 2nd ed. (Taylor & Francis, London, 1991).
- [2] D. J. Jacobs and M. F. Thorpe, "Generic rigidity percolation: The pebble game," *Phys. Rev. Lett.* **75**, 4051–4054 (1995).
- [3] D. J. Jacobs and M. F. Thorpe, "Generic rigidity percolation in two dimensions," *Phys. Rev. E* **53**, 3682–3693 (1996).
- [4] S. Boccaletti, J.A. Almendral, S. Guan, I. Leyva, Z. Liu, I. Sendiña-Nadal, Z. Wang, and Y. Zou, "Explosive transitions in complex networks' structure and dynamics: Percolation and synchronization," *Phys. Rep.* **660**, 1–94 (2016).
- [5] Abbas Ali Saberi, "Recent advances in percolation theory and its applications," *Phys. Rep.* **578**, 1–32 (2015).
- [6] Dimitris Achlioptas, Raissa M. D'Souza, and Joel Spencer, "Explosive percolation in random networks," *Science* **323**, 1453–1455 (2009).
- [7] Robert M. Ziff, "Explosive growth in biased dynamic percolation on two-dimensional regular lattice networks," *Phys. Rev. Lett.* **103**, 045701 (2009).
- [8] Robert M. Ziff, "Scaling behavior of explosive percolation on the square lattice," *Phys. Rev. E* **82**, 051105 (2010).
- [9] Y. S. Cho, J. S. Kim, J. Park, B. Kahng, and D. Kim, "Percolation transitions in scale-free networks under the achlioptas process," *Phys. Rev. Lett.* **103**, 135702 (2009).
- [10] Filippo Radicchi and Santo Fortunato, "Explosive percolation in scale-free networks," *Phys. Rev. Lett.* **103**, 168701 (2009).
- [11] Eric J. Friedman and Adam S. Landsberg, "Construction and analysis of random networks with explosive percolation," *Phys. Rev. Lett.* **103**, 255701 (2009).
- [12] R. A. da Costa, S. N. Dorogovtsev, A. V. Goltsev, and J. F. F. Mendes, "Explosive percolation transition is actually continuous," *Phys. Rev. Lett.* **105**, 255701 (2010).

- [13] Raissa M. D'Souza and Michael Mitzenmacher, "Local cluster aggregation models of explosive percolation," *Phys. Rev. Lett.* **104**, 195702 (2010).
- [14] Jan Nagler, Anna Levina, and Marc Timme, "Impact of single links in competitive percolation," *Nat. Phys.* **7**, 265–270 (2011).
- [15] Oliver Riordan and Lutz Warnke, "Achlioptas processes are not always self-averaging," *Phys. Rev. E* **86**, 011129 (2012).
- [16] Filippo Radicchi and Santo Fortunato, "Explosive percolation: A numerical analysis," *Phys. Rev. E* **81**, 036110 (2010).
- [17] Y. S. Cho and B. Kahng, "Suppression effect on explosive percolation," *Phys. Rev. Lett.* **107**, 275703 (2011).
- [18] Hyun Keun Lee, Beom Jun Kim, and Hyunggyu Park, "Continuity of the explosive percolation transition," *Phys. Rev. E* **84**, 020101(R) (2011).
- [19] Peter Grassberger, Claire Christensen, Golnoosh Bizhani, Seung-Woo Son, and Maya Paczuski, "Explosive percolation is continuous, but with unusual finite size behavior," *Phys. Rev. Lett.* **106**, 225701 (2011).
- [20] Oliver Riordan and Lutz Warnke, "Explosive percolation is continuous," *Science* **333**, 322–324 (2011).
- [21] R. A. da Costa, S. N. Dorogovtsev, A. V. Goltsev, and J. F. F. Mendes, "Critical exponents of the explosive percolation transition," *Phys. Rev. E* **89**, 042148 (2014).
- [22] Raissa M. D'Souza and Jan Nagler, "Anomalous critical and supercritical phenomena in explosive percolation," *Nat. Phys.* **11**, 531–538 (2015).
- [23] The standard definition of the fractal dimension d_f^* is as $C_1 \sim L^{d_f^*}$, where L is the length of hypercubic lattices. Because of the absent of system length in random graphs, we define the fractal dimension as $C_1 \sim N^{d_f}$. For a hypercubic lattice, we have $N = L^d$, and thus $d_f = d_f^*/d$, where d is the system dimension.
- [24] Liang Tian and Da-Ning Shi, "The nature of explosive percolation phase transition," *Phys. Lett. A* **376**, 286–289 (2012).
- [25] Y. S. Cho, S.-W. Kim, J. D. Noh, B. Kahng, and D. Kim, "Finite-size scaling theory for explosive percolation transitions," *Phys. Rev. E* **82**, 042102 (2010).
- [26] Jiantong Li and Mikael Östling, "Corrected finite-size scaling in percolation," *Phys. Rev. E* **86**, 040105(R) (2012).
- [27] Jingfang Fan, Maoxin Liu, Liangsheng Li, and Xiaosong Chen, "Continuous percolation phase transitions of random networks under a generalized achlioptas process," *Phys. Rev. E* **85**, 061110 (2012).
- [28] Jingfang Fan, Jun Meng, Yang Liu, Abbas Ali Saberi, Jürgen Kurths, and Jan Nagler, "Universal gap scaling in percolation," *Nat. Phys.* **16**, 455–461 (2020).
- [29] Nikolaos Bastas, Kosmas Kosmidis, and Panos Argyrakis, "Explosive site percolation and finite-size hysteresis," *Phys. Rev. E* **84**, 066112 (2011).
- [30] S. S. Manna and Arnab Chatterjee, "A new route to explosive percolation," *Physica A* **390**, 177–182 (2011).
- [31] Mohadeseh Feshanjerdi and Abbas Ali Saberi, "Universality class of epidemic percolation transitions driven by random walks," *Phys. Rev. E* **104**, 064125 (2021).
- [32] Detailed simulations and data analyses for different bond-insertion rules and different spatial dimensions are in progress.
- [33] Qianqian Wu and Junfeng Wang, "Thresholds and critical exponents of explosive bond percolation on the square lattice," *Int. J. Mod. Phys. C* **33**, 2250096 (2022).
- [34] Karim Bernardet, Ferenc Pázmándi, and G. G. Batrouni, "Disorder averaging and finite-size scaling," *Phys. Rev. Lett.* **84**, 4477–4480 (2000).